ACS OMEGA

Article

Cite This: ACS Omega 2019, 4, 6585−6596

http://pubs.acs.org/journal/acsodf

Phenyldihydropyrazolones as Novel Lead Compounds Against *Trypanosoma cruzi*

Maarten Sijm,[†] Julianna Siciliano de Araújo,[‡] Stefan Kunz,[†] Susanne Schroeder,[§] Ewald Edink,[†] Kristina M. Orrling,[†] An Matheeussen,[∥] Tiffany van de Meer,[†] Payman Sadek,[†] Hans Custers,[†] Ignacio Cotillo,[⊥] Julio J. Martin,[⊥] Marco Siderius,[†] Louis Maes,[∥] David G. Brown,[§] Maria de Nazaré Correia Soeiro,[‡] GeertJan Sterk,[†] Iwan J.P. de Esch,[†] and Rob Leurs*[,†]

[†]Division of Medicinal Chemistry, Faculty of Sciences, Amsterdam Institute for Molecules, Medicines and Systems (AIMMS), Vrije Universiteit Amsterdam, De Boelelaan 1108, 1081 HZ Amsterdam, The Netherlands

[‡]Laboratório de Biologia Celular, Oswaldo Cruz Institute (Fiocruz), Av. Brasil, 4365—Manguinhos, RJ, 21040-900 Rio de Janeiro, Brazil

[§]School of Biosciences, University of Kent, Canterbury CT2 7NJ, U.K.

[∥]Laboratory for Microbiology, Parasitology and Hygiene (LMPH), University of Antwerp, Universiteitsplein 1, 2610 Antwerpen, Belgium

[⊥]Diseases of the Developing World, GlaxoSmithKline, Calle de Severo Ochoa, 2, 28760 Tres Cantos, Madrid, Spain

Supporting Information

ABSTRACT: As over 6 million people are infected with Chagas disease and only limited therapeutic options are available, there is an urgent need for novel drugs. The involvement of cyclic nucleotide phosphodiesterases (PDE) in the lifecycle and biological fitness of a number of protozoan parasites has been described and several of these enzymes are thought to be viable drug targets. Within this context, a PDE-focused library was screened for its ability to affect the viability of *Trypanosoma cruzi* parasites. 5-(3-(Benzyloxy)-4-methoxyphenyl)-2-isopropyl-4,4-dimethyl-2,4-dihydro-3*H*-pyrazol-3-one (**4**), previously reported as a human PDE4 inhibitor, was identified as a hit. Upon optimization on three positions of the phenylpyrazolone scaffold, 2-isopropyl-5-(4-methoxy-3-(pyridin-3-yl)phenyl)-4,4-dimethyl-2,4-dihydro-3*H*-pyrazol-3-one (**34**) proved to be the most active compound against intracellular forms of *T. cruzi* (pIC_{50} = 6.4) with a 100-fold selectivity with respect to toxicity toward human MRC-5 cells. Evaluation on different life stages and clinically relevant *T. cruzi* strains revealed that the phenylpyrazolones are not active against the bloodstream form of the Y strain but show submicromolar activity against the intracellular form of the Y- and Tulahuen strains as well as against the nitro-drug-resistant Colombiana strain. In vitro screening of phenylpyrazolones against TcrPDEB1, TcrPDEC, and TcrCYP51 showed that there was a poor correlation between enzyme inhibition and the observed phenotypic effect. Among the most potent compounds, both TcrCYP51 and non-TcrCYP51 inhibitors are identified, which were both equally able to inhibit *T. cruzi* in vitro.

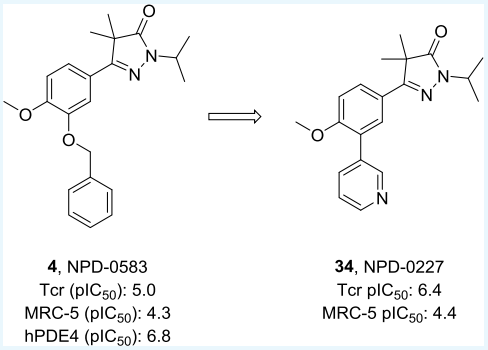

INTRODUCTION

Trypanosoma cruzi, a protozoan parasite, is the causative agent of Chagas disease.[1] This disease was once only endemic in Latin-America, however as human mobility increases it is now spreading into other areas such as Europe, Australia, Northern-America, and Middle America.[2−5] It is estimated that approximately 6 million people are currently infected worldwide.[6] Of all individuals carrying this infection about 30% will develop a progressive chronic cardiomyopathy and another 10% will develop digestive, neurological, or mixed clinical symptoms.[7]

While the current drugs benznidazole (Radanil) (**1**, Figure 1) and nifurtimox (Lampit) (**2**) are quite effective in curing the disease in its initial acute phase, efficacy of these drugs during the chronic disease phase is much less evident.[8] The recent BENEFIT trial on the efficacy of benznidazole (**1**) in patients with chronic Chagas disease reported that the cardiac deterioration was not significantly impaired, despite the significantly reduced serum parasitemia.[9] Moreover, besides their limited efficacy in the chronic phase, both benznidazole (**1**) and nifurtimox (**2**) exhibit severe side effects, require long drug administration, and are ineffective against naturally resistant *T. cruzi* strains.[10,11] Despite these risks and limitations and its relatively high disease burden, the drug discovery

Received: October 31, 2018
Accepted: April 1, 2019
Published: April 10, 2019

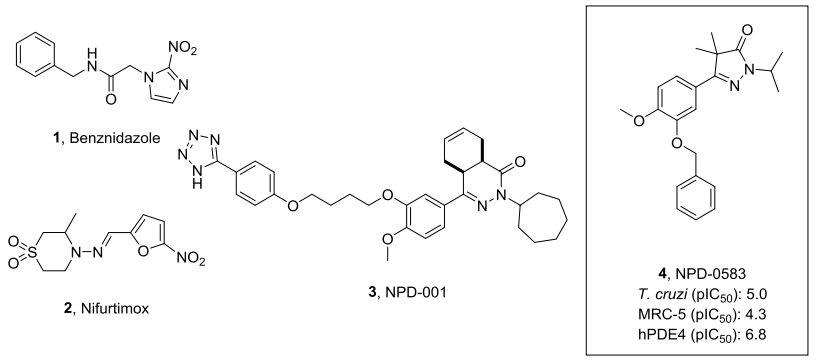

Figure 1. Current drugs against *T. cruzi*: benznidazole (**1**), nifurtimox (**2**), PDE inhibitor NPD-001 (**3**), which is able to kill *T. brucei,* and phenyldihydropyrazolone NPD-0583 (**4**) hit from the phenotypic screening.

pipeline for Chagas disease does not provide high hopes for a novel treatment on a short term notice.[12]

Mainly academic groups have been trying to fill this innovation gap, although there are some collaborations with industry in public-private partnerships.[13−15] In this paper, we describe part of the research of the EU-funded, public-private consortium PDE4NPD (www.PDE4NPD.eu), that focuses on 3′5′-cyclic nucleotide phosphodiesterases (PDEs) as targets against a number of neglected tropical diseases. PDEs are enzymes that hydrolyze phosphodiesterase bonds such as those found in the intracellular (IC) cyclic nucleotides cAMP and cGMP and thereby are involved in the control of IC signalling.[16] Level control of the secondary messengers cAMP and cGMP is essential in various cell functions, for example differentiation, proliferation, and regulation of osmotic stress in a variety of cells, including parasites.[17−19] In kinetoplastida, four different PDE families have been identified, namely PDEA-PDED, which show high homology between the different kinetoplastid species.[20]

Previously, the effectiveness of targeting parasite PDEs has been shown for *Giardia lamblia* and the closely related protozoan parasite *Trypanosoma brucei*.[21−23] An inhibitor of two parasite PDEs TbrPDEB1 and TbrPDEB2, NPD-001 (**3**, Figure 1; also disclosed as a human PDE4 inhibitor), elevated IC cAMP levels, disrupted regulation of the cell cycle, and ultimately lead to death of the trypanosomes.[24,25] Moreover, the importance of PDEs in controlling cAMP levels and thereby regulating cellular processes such as regulatory volume control in *T. cruzi* has been reported.[26−28] One of the PDE family members, TcrPDEC, has subsequently been suggested as an antiparasitic drug target.[29]

As PDE inhibition seems a viable approach toward new treatments against kinetoplastids, an in-house library of known PDE inhibitors was screened against *T. cruzi* in phenotypic assays. In this screening effort, the human PDE4 inhibitor (hPDE4 pIC_{50} = 6.8) NPD-0583 (**4**, Figure 1), previously also reported by Orrling et al. as TbrPDEB1 inhibitor (pIC_{50} = 5.4), was identified as a hit against the IC form of *T. cruzi* (pIC_{50} = 5.0).[21] On the basis of these results, three positions of the core scaffold were selected for optimization: the benzyloxy moiety R_1, the pyrazolone nitrogen substituent R_2, and the methoxy moiety on R_3 (**5**, Figure 2).

CHEMISTRY

For hit optimization and SAR analysis, we designed a synthetic route that allowed efficient modification at all three positions. Orrling et al.[21] reported a similar route for this chemical class;

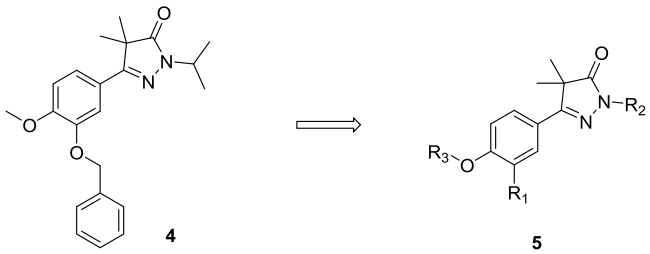

Figure 2. Hit molecule NPD-0583 (**4**) from which the phenylpyrazolone scaffold **5** was derived for further SAR (structure−activity relationship) exploration.

however, some small modifications were made to the first three steps.

In the first step, the acid chloride of benzoic acid **6** was formed and subsequently condensed with the separately formed lithium enolate of methylisobutyrate (Scheme 1). The resulting *β*-keto-ester **7** was used crude for the ring closure with hydrazine to give key intermediate **8** in 89% yield over two steps. With dihydropyrazolone **8** at hand, the first substituent of choice could be introduced on the pyrazolone nitrogen (R_2) via an alkylation with the desired aliphatic bromine. These N-alkylated intermediates (**9−21**, Scheme 1) were used in either a Suzuki reaction to install the final aryl substituent (R_1) (**22−47**, **51−64**, Scheme 1) or in a Buchwald reaction to install aliphatic amines (**48−50**). The third and final position (R_3) could be modified after demethylation of intermediate **11** (5-(3-bromo-4-methoxyphenyl)-2-isopropyl-4,4-dimethyl-2,4-dihydro-3*H*-pyrazol-3-one), followed by subsequent O-alkylation. The newly obtained *O*-alkyl intermediates (**66−74**, Scheme 1) were used in a Suzuki reaction to install the final aryl substituent (R_1), (**75−83**).

PHARMACOLOGY AND PARASITOLOGY

All compounds were initially tested for their trypanocidal activity against IC forms of *T. cruzi,* Tulahuen CL2, *β*-galactosidase strain (drug sensitive strain, (discrete typing units, DTU VI)) as well as for cytotoxicity on MRC-5_{SV2} cells (human lung fibroblasts). In-depth pharmacological profiling was performed using IC amastigotes from the naturally highly and moderately nitro-drug-resistant Colombiana strain (DTU I) and from the Y-strain (DTU II), respectively. Additionally, bloodstream trypomastigotes (BT) of the Y-strain obtained from infected Swiss Webster mice were used. Toxicity profiling was done using primary cell cultures of mouse embryonic cardiac cells. TcrCYP51 inhibition assays were performed

DOI: 10.1021/acsomega.8b02847
ACS Omega 2019, 4, 6585−6596

Scheme 1[a]

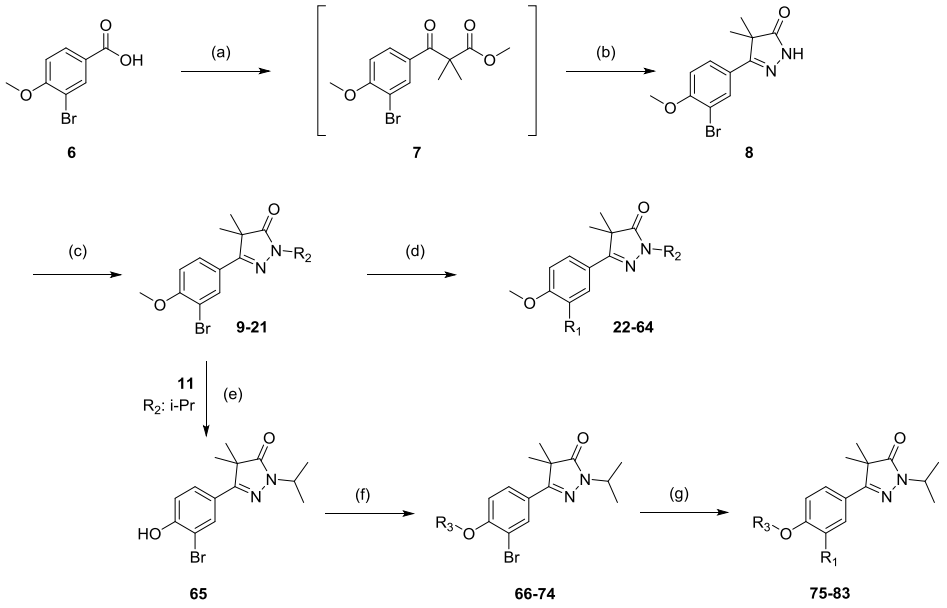

[a]Reagents and Conditions: (a) (i): ($COCl_2$), DMF, DCM, 2 h, rt, (ii): methylisobutyrate, LDA, THF, −78 °C to rt; (b) $N_2H_4{\cdot}H_2O$, EtOH, 18 h, rt; 89% Over Two Steps; (c) NaH, R_2-Br, DMF, 2 h, 50 °C; 70−95%; (d) R_1-B(OH_2), Pd(dppf)$Cl_2{\cdot}CH_2Cl_2$, 1 M Na_2CO_3, DME, 1 h, 120 °C μW; 14−94%; (e) **11**, BBr_3, DCM, 18 h, rt; 90%; (f) R_3-Br, DMF, 3 h, 50 °C; 17−96%; (g) R_1-B(OH_2), Pd(dppf)$Cl_2{\cdot}CH_2Cl_2$, 1 M Na_2CO_3, DME, 1 h, 120 °C μW; 30−94%

using CYP51 (full length) from the Tulahuen strain using the fluorescence based assay reported by Riley et al.[30] The catalytic domains of Tcr(Y)PDEC (aa 270−614) and Tcr(Y)PDEB1 (aa 564−918) were amplified by PCR from full length sequences and cloned (NdeI and XhoI) into the vector pET28a.[31] Protein production and purification of both Tcr(Y)PDE_CDs were performed following the same protocol. *Escherichia coli* strain BL21(DE3)*pLysS was transformed with either plasmid pET28aTcr(Y)PDEC_270-614 or pET28aTcr(Y)PDEB1_564-918 and the resulting recombinant strains were grown in 2YT medium at 37 °C. A typical purification yielded about 10 mg Tcr(Y)PDEC_CD and 7 mg Tcr(Y)PDEB1_CD from a 1 L cell culture. PDE activity assays are performed using the PDELight HTS cAMP phosphodiesterase kit (Lonza, Walkersville, USA).

RESULTS AND DISCUSSION

Compounds from an in-house PDE-focused library were screened in vitro for their trypanocidal effect against the IC form of *T. cruzi* (Tulahuen CL2 strain transfected with β-galactosidase gene) and their toxicity on human lung fibroblasts (MRC-5). NPD-0583 (**4**) was identified as a "hit" from which the phenyl-pyrazolone scaffold (**5**, Figure 2) was derived for further optimization. As the catechol moiety of NPD-0583 (**4**) is a chemotype commonly observed in human PDE4 inhibitors, and human PDE off-target activity is preferably avoided, the first analogues synthesized did not contain the 3-benzyloxy moiety. Instead, the phenyl group was attached directly to the pyrazolone-phenyl scaffold, leading to compound **22** (Table 1), which has a similar activity as NPD-0583 (**4**) with a pIC_{50} of 5.1. Moreover, substituted phenyl analogues (**23**−**32**, Table 1) showed a similar or improved activity over NPD-0583 (**4**, Figure 1). While introduction of a 2-fluorophenyl (**23**) led to diminished activity (pIC_{50} < 4.2), both the 3- and 4-fluorophenyl analogues (**24**−**25**, Table 1) showed a substantial increase in activity over the unsubstituted phenyl (**22**) with pIC_{50} values around 6. Introduction of a 3- and 4-chloro- or methoxyphenyl ring (**26**−**29**, Table 1) also increased activity compared to the unsubstituted phenyl analogue (**22**) with pIC_{50} values around 5.5. The most active substituted phenyl derivative was the 3-cyanophenyl-substituted compound (**30**) with a pIC_{50} of 6.4, while the 4-cyanophenyl analogue (**31**, Table 1) had an activity of 5.6. Substituting both the 3- and 4-position, as seen with dimethoxyphenyl **32** did not improve activity (pIC_{50} = 4.9, Table 1).

Introduction of pyridines on the R_1 position led to mixed results. The 2-pyridine analogue **33** (Table 1) showed almost no activity, while the 3- and 4-pyridine substituted phenyldihydropyrazolones (**34**−**35**) were amongst the most potent analogues with pIC_{50} values of 6.4 and 5.8, respectively. Introduction of a fluorine on the 4-position of the 3-pyridine (**36**) did not affect the activity, while substitution with larger substituents such as 4-methyl (**37**), 4-methoxy (**38**), and 4-cyano (**39**) resulted in a 10-fold decrease in potency (Table 1). Introduction of a methyl group on the 6-position of the 3-pyridinyl moiety (**40**) decreased activity even further. Adding a small substituent on the 3-position of 4-pyridines resulted in a significant increase in activity; the 3-fluoro-4-pyridinyl analogue (**41**, Table 1) is for example very active with a pIC_{50} of 6.3, while the 3-methyl-4-pyridinyl (**42**) analogue has a pIC_{50} of 6.4, as opposed to 5.8 for the unsubstituted 4-pyridinyl (**35**). These activities are similar to 3-pyridinyl-phenylpyrazolone **34** (pIC_{50} = 6.4), the most potent compound in the series obtained so far. Introduction of other heterocycles such as a pyrimidine (**43**, Table 1), indole (**44**), isoquinoline (**45**), furan (**46**), and thiophene (**47**) generally caused a large decrease in activity, exception being pyrimidine **43** which only showed a minor decrease in activity (pIC_{50} = 6.0) compared to the 3-pyridine substituted phenylpyrazolone **34**.

DOI: 10.1021/acsomega.8b02847
ACS Omega 2019, 4, 6585−6596

Table 1. Phenotypic Activity against IC Amastigotes of *T. cruzi* (Tulahuen Strain) and on MRC-5 Cell Growth by Phenyldihydropyrazolones with Modification on the R_1 Position

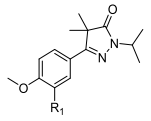

Compd	R_1	*T.cr* (pIC_{50})[a]	MRC-5 (pIC_{50})[a]	Compd	R_1	*T.cr* (pIC_{50})[a]	MRC-5 (pIC_{50})[a]
4	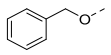	5.0	4.3	**32**	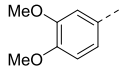	4.9	4.5
22		5.1	<4.2	**33**		4.6	<4.2
23		<4.2	<4.2	**34** NPD-0227		6.4	4.4
24	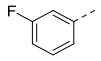	5.9	4.5	**35**		5.8	<4.2
25	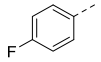	6.0	4.4	**36**	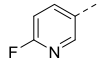	6.3	4.3
26	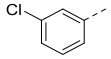	5.6	5.0	**37**	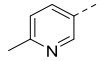	5.5	4.4
27	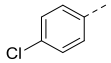	5.6	5.1	**38**	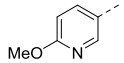	5.6	4.5
28	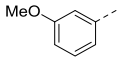	5.6	4.6	**39**	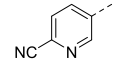	5.4	<4.2
29	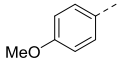	5.4	5.2	**40**		4.8	<4.2
30	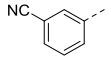	6.4	4.6	**41**		6.3	4.7
31	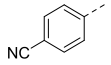	5.6	4.4	**42**	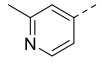	6.4	5.0

[a]All reported values are within a standard deviation of ±0.2.

Table 2. Phenotypic Activity against IC Amastigotes of *T. cruzi* (Tulahuen Strain) and on MRC-5 Cell Growth by Phenyldihydropyrazolones with Modification on the R_2 Position

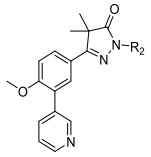

Compd	R_2	*T.cr* (pIC_{50})[a]	MRC-5 (pIC_{50})[a]	Compd	R_2	*T.cr* (pIC_{50})[a]	MRC-5 (pIC_{50})[a]
51		4.4	<4.2	**58**		5.7	4.9
52		4.6	<4.2	**59**	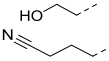	4.3	<4.2
53		5.4	<4.2	**60**		5.4	<4.2
34 (NPD-0227)		6.4	4.4	**61**	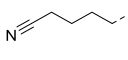	5.9	<4.2
54		6.2	4.6	**62**	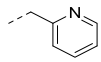	5.0	<4.2
55		6.4	4.6	**63**	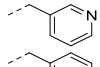	5.3	<4.2
56		6.0	4.5	**64**	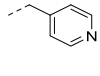	5.8	<4.2
57		6.5	4.7				

[a]All reported values are within a standard deviation of ±0.2.

DOI: 10.1021/acsomega.8b02847
ACS Omega 2019, 4, 6585−6596

Table 3. Phenotypic Activity against IC Amastigotes of *T. cruzi* (Tulahuen Strain) and on MRC-5 Cell Growth by Phenyldihydropyrazolones with Modification on the R_3 Position

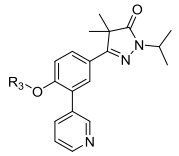

Compd	R_3	*T.cr* (pIC_{50})[a]	MRC-5 (pIC_{50})[a]	Compd	R_3	*T.cr* (pIC_{50})[a]	MRC-5 (pIC_{50})[a]
34 (NPD-0227)		6.4	4.4	**79**		5.6	<4.2
75		5.0	4.5	**80**		5.1	4.7
76		5.1	4.6	**81**		5.0	<4.2
77		6.0	4.6	**82**		4.4	<4.2
78		6.1	5.2	**83**		4.9	4.4

[a]All reported values are within a standard deviation of ±0.2.

To extend the SAR on this position, several non-aromatic heterocycles (**48**−**50**, Table 1) were introduced on the R_1 position, but the activity was 100-fold lower than the most potent hits obtained so far, showing that an aromatic feature is preferred on this position.

In the obtained set of phenyldihydropyrazolones with different R_1 substituents, several compounds show potencies around 6.4 (pIC_{50}). Since 3-pyridinyl **34** (NPD-0227) has the lowest clog *P*, low MRC-5 toxicity, and does not contain a fluorine moiety that has the potential risk of nucleophilic aromatic substitution, SAR exploration on the R_2 and R_3 position (**5**, Figure 2) was further done using this moiety on the R_1 position. Initially, the *N*-unsubstituted phenyldihydropyrazolone (**51**) as well as different sizes of branched and unbranched aliphatic chains (**52**−**58**, Table 2) were synthesized and evaluated on the R_2 position. While the non-substituted compound (**51**, Table 2) is virtually inactive with an pIC_{50} of 4.4, adding aliphatic R_2 substituents substantially increased activity. While introduction of a methyl group (**52**, Table 2) resulted only in a minor increase, the *N*-ethyl substituted dihydropyrazolone (**53**) showed a 10-fold increase in parasitic activity (pIC_{50} = 5.4). This activity was further increased by adding another methyl moiety, as in the *N*-isopropyl substituted dihydropyrazolone NPD-0227 (**34**, Table 2), which has a pIC_{50} of 6.4. Analogues containing larger alkyl groups on the R_2 position, such as cyclopropylmethyl **54**, cyclobutylmethyl **55**, isopentyl **56**, and cyclopentyl **57** all showed submicromolar antiparasitic activity (Table 2). Introduction of the larger cycloheptyl (**58**, Table 2) decreased the activity against *T. cruzi* while increasing the cytotoxicity. Introduction of a polar 2-hydroxyethyl group (**59**) on the pyrazolone nitrogen did not improve the activity compared to the unsubstituted dihydropyrazolone **51** (Table 2). Introducing butanenitrile (**60**) or pentanenitrile (**61**) led to improved activities compared to the unsubstituted pyrazolone **51** with pIC_{50} values of 5.4 and 5.9, respectively. To establish if aromatic moieties are allowed on the R_2 position, three methylpyridines (**62**−**64**, Table 2) were introduced. The observed activities were substantially higher than for the unsubstituted dihydropyrazolone (**51**). The 4-pyridinylmethyl (**64**, pIC_{50} = 5.8) showed higher activity than the 2- and 3-pyridinylmethyl analogues (**62**, **63**). However, the antiparasitic activity of the 4-pyridinylmethyl-substituted pyrazolone **64** (pIC_{50} = 5.8) was well below the activity of the isopropyl derivative **34**. Overall, variations on the R_2-position did not improve the activity significantly compared to the isopropyl dihydropyrazolone (**34**, Table 2). Although the cyclopropylmethyl (**54**), cyclobutylmethyl (**55**), and cyclopentyl (**57**) dihydropyrazolones reached similar potencies as the isopropyl (**34**), the mild increase in toxicity observed with these compounds as well as higher clog *P* values resulted in the decision to continue the SAR exploration on R_3 (**5**, Figure 2) with the *N*-isopropyl moiety on the R_2 position (**34**).

The final position that was varied on the phenylpyrazolone scaffold was the R_3 position (**5**, Figure 2). At first, small aliphatic moieties up to 5 carbons (**75**−**79**, Table 3) were introduced. While the smaller ethyl (**75**) and isopropyl (**76**) substituents showed a quite drastic drop in activity compared to the original methyl-substituted phenylpyrazolone (**34**) (Table 3), the slightly larger cyclopropylmethyl (**77**), cyclobutylmethyl (**78**), and cyclopentyl (**79**) are equipotent to the methoxy analogue (**34**) with pIC_{50} values around 6.3. Installing the larger benzyl group (**80**) caused a larger drop in activity (pIC_{50} of 5.1).

In order to decrease the log *P*, several aliphatic moieties with heteroatoms were installed. However, neither acetonitrile (**81**), tetrahydrofuran (**82**), or tetrahydropyran (**83**) moieties proved to provide a positive effect on activity (Table 3) as all these derivatives displayed a pIC_{50} of 5.0 or lower. Hence, the methoxy group, already present in the original hit, remains the substituent of choice.

After SAR-investigation on the three selected positions (**5**, Figure 2), the most optimal compound within these series contained a 3-pyridinyl moiety on R_1, an isopropyl group on the R_2 position, and a methyl substituent on the R_3 position. The most active hit, the cyclopentyl-substituted phenyldihydropyrazolone (**57**, Table 2), was ∼32 fold more active than the original hit (**4**, Figure 1). Nonetheless, it was decided to continue further studies with the 3-pyridinyl phenyldihydropyrazolone (**34**, NPD-0227) as it showed a slightly lower cytotoxicity (∼100 fold selectivity) and generally had more favorable physicochemical properties compared to the

DOI: 10.1021/acsomega.8b02847
ACS Omega 2019, 4, 6585−6596

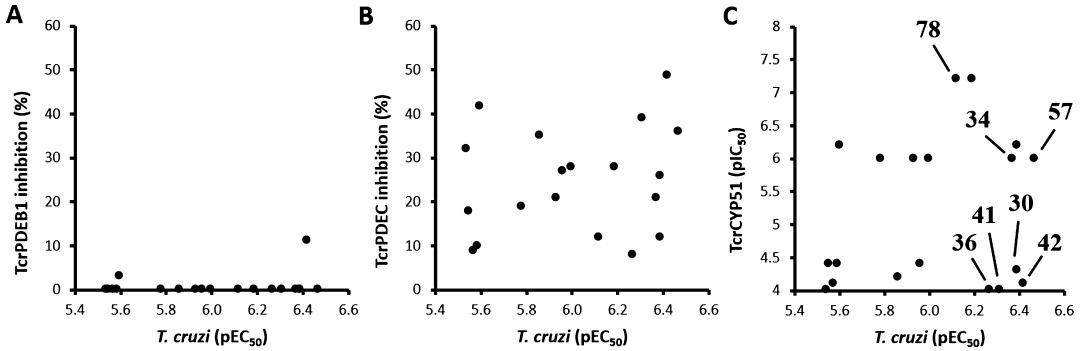

Figure 3. Measured biochemical evaluation activities of selected phenylpyrazolones correlate poorly with the phenotypic activity. (A) TcrPDEB1 inhibition at 10 μM (%) against the phenotypic inhibition on *T. cruzi* (pIC_{50}). (B) TcrPDEC inhibition at 10 μM (%) against the phenotypic inhibition on *T. cruzi* (pIC_{50}). (C) TcrCYP51 inhibition (pIC_{50}) against phenotypic inhibition on *T. cruzi* (pIC_{50}). Raw data can be found in Table S1.

Table 4. In Depth in Vitro Parasitology against BT of the Y-Strain (DTU II) and IC Amastigotes of the Tulahuen Strain (DTUs VI)

cmpnd	pIC_{50} *T. cruzi* (Tulahuen, IC) (96 h)[a]	pIC_{50} *T. cruzi* (Y-strain, BT) (24 h)[a]	*T. cruzi* CYP51 (pIC50)[a]	clog *P*[b]	clog *S*[b]	TPSA (Å)[b]
3	5.6	4.9	N.D.	1.3	−2.9	90
30	6.2	4.3	4.3	4.5	−5.9	66
34	6.4	<4.3	6.0	3.4	−4.5	55
36	6.3	4.3	4.0	4.0	−5.5	55
41	6.4	4.3	4.0	4.0	−5.5	55
42	6.2	4.3	4.1	3.6	−4.7	55
57	6.4	4.5	6.0	4.0	−5.1	55
78	6.0	3.9	7.2	4.7	−6.0	55

[a]All reported values are within a standard deviation of ±0.2. [b]clog *P*, clog *P*, and TPSA are calculated using CDD Vault.

other equipotent analogues. The role of physicochemical properties was further investigated by plotting the *T. cruzi* pIC_{50}'s against clog *P*, clog *S*, and TPSA. However, correlations were all poor with R^2's below 0.15 (Table S1, Figures S1−S3).

BIOCHEMICAL EVALUATION OF SELECTED PHENYLDIHYDROPYRAZOLONES

As the hit originated from a PDE-focused library and was a moderately potent human PDE4 and TbrPDEB1 inhibitor, the possibility that these molecules exert their phenotypic effect via *T. cruzi* PDEs was explored. Additionally, compounds were screened for their activity against TcrCYP51 as the 3-pyridinyl moiety is a common chemotype for this known drug target.[32]

Analysis of PDE expression in *T. cruzi* based on the transcriptome data of Li et al. show that all five trypanosome PDEs (A, B1/B2, C, and D) are expressed in trypamastigotes, next to TcrCYP51.[33] Expression levels of TcrPDEC and TcrCYP51 do not change more than two-fold after in vitro infection of human cells, while the mRNA concentrations of TcrPDEB1 and B2 were significantly (log 2 fold-change > 1; *q*-value < 0.05) downregulated during the amastigote developmental stages (Supporting Information Figure S4). In epimastigotes (insect stage), only TcrPDEC was upregulated compared to trypomastigotes (log 2 fold-change = 2.7; *q*-value = 1.7×10^{-10}) (Figure S4).[33]

As mentioned, PDEB1 and PDEB2 of *T. brucei* have been shown to be essential for survival of the parasite.[34] While not much is yet known about the role of the *T. cruzi* PDEB enzymes, its homology with the essential PDEB enzymes of *T. brucei* led to the hypothesis that TcrPDEB inhibition may be the underlying mechanism of the phenotypic activity of the phenyldihydropyrazolones. Therefore, the TcrPDEB1 catalytic domain was expressed and purified and selected molecules from the phenylpyrazolone series were evaluated for inhibitory potential of this enzyme in an in vitro activity assay (Figure 3A). Overall, the activity was very poor; for example, 3-methyl-4-pyridinyl-substituted phenylpyrazolone **42** (pIC_{50} *T. cruzi* = 6.4) inhibited 11% at 10 μM, while NPD-0227 (**34**, pIC_{50} *T. cruzi* = 6.4) did not show any TcrPDEB1 inhibition at all, making it unlikely that this enzyme is responsible for the observed phenotypic effect.

TcrPDEC was previously reported as a biochemically validated target by King-Keller et al.; hence, a selection of phenylpyrazolones was tested for their inhibition of the activity of the TcrPDEC catalytic domain (a.a. 270−614).[29,31] Overall, the inhibitory activity of the phenyl-dihydropyrazolones against TcrPDEC-CD proved to be relatively weak (Figure 3B). The most potent phenotypic hits show less than 50% inhibition of TcrPDEC-CD at 10 μM. For example, 3-methyl-4-pyridinyl substituted phenylpyrazolone **42** inhibits 49% (pIC_{50} *T. cruzi* = 6.4, Table 1) and NPD-0227 (**34**) only 21% of TcrPDEC-CD activity (pIC_{50} *T. cruzi* = 6.4). The poor correlation between the phenotypic activity and TcrPDEC-CD inhibition of this series suggests that this enzyme is also not a key mediator in the observed phenotypic effect (Figure 3B).

Inhibition of TcrCYP51 has previously been shown to lead to antiparasitic effects in vitro and in vivo.[35−37] Yet, the recent posacanozole trial suggests that the azole-based TcrCYP51 inhibitor combined with benznidazole is not able to cure parasitemia.[38] These findings have led to a serious debate on the validity of TcrCYP51 as drug target.[37−44] However, in the posacanozole trial, the used dosage of the TcrCYP51 inhibitor only corresponds to 10−20% of the curative dose in mice.[39,41] Moreover, the trial also employed a short treatment regimen,

DOI: 10.1021/acsomega.8b02847
ACS Omega 2019, 4, 6585−6596

whereas it is also known that TcrCYP51 inhibitors are slow trypanocidal compounds.[39,41,42] It has been suggested that with the design of specific TcrCYP51 inhibitors, instead of repurposing fungal CYP51 inhibitors, different combination therapies, or longer treatment regimens, TcrCYP51 inhibition still has potential.[37,41,42,45] In order to investigate whether the observed antiparasitic effect of the newly identified hit series is caused by inhibition of TcrCYP51, a selection of inhibitors was screened against this enzyme. Gunatilleke et al. reported commonly observed scaffolds in the screening against TcrCYP51: amongst their top 185 ranked hits, 92 contained a 3-pyridinyl and 67 contained a 4-pyridinyl moiety, which is true for most compounds in the phenylpyrazolone series.[32] Interestingly, two distinct groups are visible in Figure 3C while all compounds show phenotypic activity, one group showed pIC_{50} values >6.0 against CYP51, while the other group is virtually inactive. For example, NPD-0227 (**34**) inhibits TcrCYP51 with a pIC_{50} of 6.0 (pIC_{50} *T. cruzi* = 6.4), while 4-fluoro-3-pyridinyl substituted phenylpyrazolone **36** (NPD-0398; pIC_{50} *T. cruzi* = 6.3) has a pIC_{50} of 4.0 on this enzyme (Figure 3C, Table 4). Also, compounds **30**, **41**, and **42** are similarly inactive against TcrCYP51, while still showing a submicromolar potency against *T. cruzi*.

IN-DEPTH IN VITRO PARASITOLOGICAL EVALUATION

Next, several of the most active phenylpyrazolones were tested more in-depth for their antiparasitic action. BT from the Y-strain (DTU II) and IC amastigotes of the Tulahuen, Y and Colombiana strains (DTUs VI, II, and I) were used.[46] All compounds show (sub)micromolar activities against the amastigotes from the Tulahuen strain, but both TcrCYP51 actives (compounds **34**, **57**, **78**, Figure 3C, Table 4) as well as the inactives **30**, **36** (NPD-0398), **41** and **42** (Figure 3C, Table 4) showed a similar drop in activity between the bloodstream form and the IC forms. Such a difference in phenotypic activity is observed more often and has been hypothesized to be an issue for TcrCYP51 inhibitors.[36,47] Yet, in the current phenylpyrazolone series this difference in phenotypic activity is also seen for compounds without TcCYP51 inhibitory activity. Since all compounds have similar physicochemical properties (Table 4) and will thus have most likely similar cellular penetration, another unidentified mechanism of action is responsible for the observed phenotypic effects.

Screening of NPD-0227 (**34**) against the IC form of the nitro-drug-resistant strains, the Y and Colombiana showed pIC_{50}'s of 7.0 and 6.3, respectively (Table S3). Also, this compound did not present a cardiotoxic profile, leading to high selectivity indexes (SI) when amastigotes from the different strains were assessed inside cardiac cell cultures (Table S3).

CONCLUSIONS

By screening a PDE focused library for anti-*T. cruzi* compounds, phenyldihydropyrazolone **4** was identified as a starting point for further hit optimization. From this structure, the phenylpyrazolone scaffold (**5**, Figure 2) was derived and optimized at three different positions. Investigation of the R_1 position led to the discovery of 3-pyridinyl-phenyldihydropyrazolone **34** (NPD-0227) as the best in this series, showing a pIC_{50} of 6.4 and 100-fold selectivity over human MRC-5 cells and >476-fold selectivity over cardiac cell cultures. Although the SAR investigation on the R_2 and R_3 positions (**5**, Figure 2) yielded useful SAR data, activities did not improve compared to the initial hit. Screening of a selection of phenylpyrazolones on TcrPDEC and TcrPDEB1 showed low activities and poor correlation with phenotypic inhibition, suggesting that neither of these PDEs is responsible for the observed phenotypic activity. In vitro screening of phenylpyrazolones against TcrCYP51 showed both active and inactive compounds. Parasitic screening of both CYP51 actives (**34**, **57** and **78**) and inactives (**30**, **36**, **41** and **42**) indicates that inhibition of this enzyme is not responsible for the observed phenotypic action of this class of compounds. 3-Pyridine **34** (NPD-0227) shows improved phenotypic activity over the currently used drug benznidazole (**1**) on the IC form of the Tulahuen and Y-strain of *T. cruzi* (pIC_{50} = 6.4 and 7.0 respectively) as well as against the highly nitro-drug-resistant Colombiana strain (pIC_{50} = 6.3). The low activity of this series on the bloodstream form will likely prevent full sterile cure. Additional research is needed to improve the activity against the bloodstream form and/or evaluate this class of compounds for combination therapy against *T. cruzi*.

EXPERIMENTAL SECTION BIOLOGY

CYP51 Assay Protocol. Assay was carried out as described in Riley et al.[30]

***T. cruzi* Cellular Assay.** BT of the Y strain of *T. cruzi* were obtained by cardiac puncture of infected Swiss Webster mice, on the parasitemia peak.[48,49] For the standard in vitro susceptibility assay on IC amastigotes, *T. cruzi* Tulahuen CL2, β-galactosidase strain (nifurtimox-sensitive), was used. The strain is maintained on MRC-5_{SV2} (human lung fibroblast) cells7 in MEM medium, supplemented with 200 mM L-glutamine, 16.5 mM $NaHCO_3$, and 5% inactivated fetal calf serum (FCSi). All cultures and assays are conducted at 37 °C under an atmosphere of 5% CO_2.

MRC-5 Cytotoxicity Cellular Assay. MRC-5 SV2 cells, originally from a human diploid lung cell line, were cultivated in MEM, supplemented with L-glutamine (20 mM), 16.5 mM sodium hydrogen carbonate, and 5% FCS. For the assay, 10^4 cells/well were seeded onto the test plates containing the prediluted sample and incubated at 37 °C and 5% CO_2 for 72 h. Cell viability was assessed fluorimetrically 4 h after addition of resazurin (excitation 550 nm, emission 590 nm). The results are expressed as percentage reduction in cell viability compared to untreated controls.

Cytotoxicity Assays on Cardiac Cells. Non-infected primary cardiac cell cultures were incubated at 37 °C for 48 h with increasing concentrations of each compound diluted in RPMI. Morphology and spontaneous contractibility were evaluated by light microscopy, and cellular viability was determined by PrestoBlue tests.[50] The results are expressed as the difference in reduction between treated and nontreated cells according to the manufacturer instructions and the LC_{50} value (minimum concentration that reduces in 50% the cellular viability) was determined.[50]

Trypanocidal Activity. BT from Y strain (5×10^6/mL) obtained from the blood of Swiss male infected mice (5×10^4 par/animal, ip) at the parasitemia peak were incubated for 24 h at 37 °C in RPMI in the presence or absence of 1:3 serial dilutions of the compounds (0−50 μM) for determination of parasite death rates through the direct quantification of live parasites by light microscopy. The EC_{50} (minimum compound concentration that reduces 50% of the number of parasites) was calculated. The more promising compounds [$EC_{50} \leq$

DOI: 10.1021/acsomega.8b02847
ACS Omega 2019, 4, 6585−6596

benznidazole (**1**)] were evaluated on IC amastigotes of the Y and Colombiana strains in infected cardiac cell cultures.[48] After 24 h infection (10:1 parasite/cell rate), the cultures were treated for 48 h at 37 °C with nontoxic concentrations of the compounds. Following the treatment, the cultures were washed with saline, fixed with Bouin for 5 min, stained with Giemsa, and evaluated by light microscopy. The percentage of infected host cells and the number of parasites per cell were determined for the calculation of the infection index, which represents the multiplication index using these two parameters, and then the pIC_{50} values were determined.[49] SI is expressed by the ratio between pLC_{50} (toxicity for mammalian cells) and the pIC_{50} (activity on the parasite).

Construction of Plasmids. The catalytic domains of Tcr(Y)PDEC (aa 270−614) and Tcr(Y)PDEB1 (aa 564−918) were amplified by PCR from full length sequences and cloned (NdeI and XhoI) into the vector pET28a. The sequences were verified by sequencing performed by GENEWIZ Inc.

Protein Production. Protein productions of both Tcr(Y)-PDE_CDs were done following the same protocol. *E. coli* BL21(DE3)*pLysS was transformed with either plasmid pET28aTcr(Y)PDEC_270-614 or pET28aTcr(Y)-PDEB1_564-918 and the resulting recombinant strains were grown in 2YT medium at 37 °C. Protein overproduction overnight at 18 °C was induced with 0.5 mM isopropyl 1-thio-β-D-galactopyranoside (IPTG) at OD_{600} = 0.6−0.8. Harvested cells were resuspended in buffer A [20 mM Tris-HCl, pH 8.0, 500 mM NaCl, 20 mM imidazole, 1 mM dithiothreitol (DTT)] and lysed by one cycle of cell disruption at 25 kpsi.

Protein Purification. Protein purification was performed at 4 °C. Cleared lysates were loaded on a 5 mL HisTrap HP column (GE Healthcare) charged with $NiSO_4$. Unbound proteins were washed off with buffer A and the protein eluted with buffer A containing 400 mM imidazole and immediately passed through a HiPrep 26/10 desalting column (GE Healthcare) equilibrated with 20 mM Tris HCl, pH 8.0, 100 mM NaCl, and 2 mM DTT. Next, the protein was subjected overnight to Thrombin cleavage (2−10 units per mg of protein) at 4 °C. Cleaved material was separated from uncleaved material by passing it through a gravity flow sepharose column charged with $NiSO_4$ and further purified by ion-exchange chromatography on Q Sepharose (5 mL HiTrap Q HP, GE Healthcare) equilibrated in buffer C (50 mM Tris HCl, pH 8.0, 100 mM NaCl, 1 mM $MgCl_2$, and 1 mM DTT). The protein was eluted with a linear gradient from 0 to 100% buffer D (50 mM Tris HCl, pH 8.0, 500 mM NaCl, 1 mM $MgCl_2$, and 1 mM DTT) over 20 column volumes. Aggregates were removed by gel filtration on a Superdex 200 Increase 10/300 GL (GE Healthcare) equilibrated in 20 mM Tris HCl, pH 7.5, 100 mM NaCl, 1 mM $MgCl_2$, and 1 mM DTT. A typical purification yielded about 10 mg Tcr(Y)PDEC_CD and 7 mg Tcr(Y)PDEB1_CDfrom a 1 L cell culture.

TcrPDEB1 and TcrPDEC Activity Assays. PDE activity assays were performed using the PDELight HTS cAMP phosphodiesterase kit (Lonza, Walkersville, USA). The assay is performed at 25 °C in nonbinding, low volume 384 wells plates (Corning, Kennebunk, ME, USA). PDE activity measurements (Tcr(Y)PDEC_CD; K_m 11.12 μM ± 1.78, Tcr(Y)PDEB1; K_m 2.22 μM ± 0,31) are made in "stimulation buffer" (50 mM Hepes, 100 mM NaCl, 10 mM MgCl, 0.5 mM EDTA, 0.05 mg/mL BSA, pH 7.5). For each PDE, the optimal enzyme concentration was determined according to the manufacturers protocol. Single concentration measurements are made at 10 μM inhibitor concentration (Triplo measurements/assay, n = 2). Dose−response curves were made in the range 100 μM to 10 pM (Triplo measurements/assay, n = 3). Compounds were diluted in dimethyl sulfoxide (DMSO) (final concentration 1%). Inhibitor dilutions (2,5 μL) were transferred to the 384-wells plate, 2, 5 μL PDE in stimulation buffer is added and mixed, 5 μL cAMP (at 2 × K_m up to 20 μM) is added, and the assay is incubated for 20 min at 300 rpm. The reaction is terminated by addition of 5 μL Lonza Stop Buffer supplemented with 10 μM NPD-0001. Next, 5 μL of Lonza Detection reagent (diluted to 80% with reaction buffer) is added, and the reaction incubated for 10 min, shaking 300 rpm. Luminescence was read with a VICTOR3 luminometer using a 0.1 s/well program.

Relative light units (RLUs) were measured in comparison to the DMSO-only control; NPD-001 was taken along as positive control. The K_i values of the inhibitors are represented as the mean of at least three independent experiments with the associated standard error of the mean (SEM).

EXPERIMENTAL SECTION CHEMISTRY

Chemicals and reagents were obtained from commercial suppliers and were used without further purification. Anhydrous dimethylformamide (DMF), tetrahydrofuan (THF), and dichloromethane (DCM) were obtained by passing them through an activated alumina column prior to use. Microwave reactions were executed using a Biotage Initiator microwave system. ^{1}H NMR spectra were recorded on a Bruker AVANCE 250 (250 MHz), Bruker AVANCE 400 (400 MHz), Bruker AVANCE 500 (500 MHz), or Bruker 600 AVANCE (600 MHz) spectrometer. Data are reported as follows: chemical shift, integration, multiplicity (s = singlet, d = doublet, dd = double doublet, t = triplet, dt = double triplet, q = quartet, p = pentet, h = heptet, bs = broad singlet, m = multiplet), and coupling constants (Hz). Chemical shifts are reported in ppm with the natural abundance of deuterium in the solvent as the internal reference ($CDCl_3$: δ 7.26, $(CD_3)_2SO$: δ 2.50). ^{13}C NMR spectra were recorded on a Bruker AVANCE 500 (126 MHz) or Bruker AVANCE 600 (150 MHz). Chemical shifts are reported in ppm with the solvent resonance resulting from incomplete deuteration as the internal reference ($CDCl_3$: δ 77.16 or $(CD_3)_2SO$: δ 39.52). Systematic names for molecules according to IUPAC rules were generated using the Chemdraw AutoName program. Liquid chromatography−mass spectroscopy (LC−MS) data were gathered using a Shimadzu HPLC/MS workstation with an LC-20AD pump system, SPD-M20A diode array detector, and LCMS-2010 EV mass spectrometer. The column used is an XBridge C18 5 μm column (100 mm × 4.6 mm). Solvents used were the following: solvent B = ACN, 0.1% formic acid; solvent A = water, 0.1% formic acid. The analysis was conducted using a flow rate of 1.0 mL/min, start 5% B, linear gradient to 90% B in 4.5 min, and then 1.5 min at 90% B, linear gradient to 5% B in 0.5 min and then 1.5 min at 5% B, total run time of 8 min. All reported compounds have purities >95%, measured at 254 nm, unless otherwise mentioned. All high-resolution mass spectroscopy (HRMS) spectra were recorded on a Bruker micrOTOF mass spectrometer using electron spray ionization (ESI) in positive-ion mode. Column purifications were either carried out automatically using Biotage equipment or manually, using 60−200 mesh silica. Thin-layer chromatography analyses were performed with Merck F254 alumina silica plates using UV visualization. All

DOI: 10.1021/acsomega.8b02847
ACS Omega 2019, 4, 6585−6596

reactions were done under an N_2 atmosphere, unless specifically mentioned.

General Methods. *General Method A: Synthesis of β-Keto-esters.* Benzoic acid **6** (25 g, 108 mmol) was suspended in DCM (50 mL) while cooling to 0 °C. Subsequently, oxalyl dichloride (13.7 mL, 162 mmol) and DMF (0.08 mL, 1.08 mmol) were added and the mixture was allowed to warm up to room temperature. The mixture was stirred for 2 h after which volatiles were evaporated. The remaining solids were redissolved in 50 mL of THF. In a separate flask, methyl isobutyrate (18.6 mL, 162 mmol) was stirred in THF (50 mL) at −78 °C and a 2 M lithium di-isopropyl amide (LDA) (65 mL, 130 mmol) was added dropwise while maintaining −78 °C. Upon full addition, the mixture was stirred for 45 min after which the acid chloride of **6** in THF was added dropwise, again maintaining the temperature at −78 °C. The reaction was allowed to warm up to room temperature after which crude was quenched with water and extracted with diethyl ether. The organic phase was washed twice with water and once with brine. The organic layer was then dried with $MgSO_4$, filtered, and evaporated to dryness. The crude was used in the next step without further purification.

General Method B: Ring Closure of β-Keto-esters. Crude keto-ester **7** (25 g, 79 mmol) was dissolved in ethanol (75 mL) and hydrazine hydrate (64%) (38.6 mL, 793 mmol) was added. The reaction was stirred at room temperature for 48 h after which white precipitation was visible. To the stirred solution, 20 mL of water was added to allow further precipitation, after which solids were filtered off. Collected solids were dried in vacuo, yielding the desired product.

General Method C: N-Alkylation of Pyrazolones. Pyrazolone **8** (10 g, 34 mmol) was dissolved in dry DMF (25 mL) and cooled to 0 °C. Sodium hydride (60% in mineral oil) (1.48 g, 37 mmol) was added, and the reaction was stirred for 30 min at room temperature after which 2-bromopropane (3.54 mL, 38 mmol) was added. The reaction was stirred for 2 h at 50 °C after which the reaction mixture was quenched with 50 mL of water. White solids precipitated after quenching, which were filtered off and washed with water (2 × 25 mL). The white solids were dried in vacuo, yielding the target compound as a white solid. On a small scale (<0.5 g), not all analogues precipitated after quenching, instead a purification over SiO_2 was done.

General Method D: Suzuki Coupling. Pyrazolone **11** (1.0 g, 3.0 mmol) and pyridin-3-ylboronic acid (0.54 g, 4.4 mmol) were charged to a microwave vial after which dimethoxyethane (DME) (12 mL) and 1 M Na_2CO_3 (8.84 mL, 8.84 mmol) were added. The mixture was degassed with N_2 for 5 min after which $Pd(dppf)Cl_2$ (120 mg, 0.15 mmol) was added. The reaction was then heated in the microwave for 1 h at 120 °C. The reaction mixture was diluted with MTBE and filtered over Celite. The residue was washed with saturated $NaHCO_3$ (2×) and brine (1×). The organic phase was dried over Na_2SO_4, filtered, and concentrated in vacuo to be further purified over SiO_2 using a gradient of 40% EtOAc in heptane toward 60% EtOAc in heptane. The target compound was obtained as a white solid.

General Method E: Buchwald Coupling. Pyrazolone **11** (50 mg, 0.15 mmol), piperidine (0.017 mL, 0.18 mmol), $Pd_2(dba)_3$ (13 mg, 0.015 mmol), Xantphos (17 mg, 0.029 mmol), and Na*t*BuO (28 mg, 0.29 mmol) were added to a microwave tube. The mixture was diluted with dry toluene (2 mL) and degassed with N_2 for 5 min. The mixture was heated in the microwave at 130 °C for 30 min. The reaction mixture was diluted with MTBE and filtered over Celite. The residue was extracted with 1 M Na_2CO_3 (2×) and brine (1×) after which the organic phase was dried over Na_2SO_4 and concentrated in vacuo. The remaining crude was purified over SiO_2 using a gradient from 50% EtOAc in *n*-heptane toward 100% EtOAc, yielding the desired product as a white solid.

General Method F: Demethylation. Pyrazolone **11** (10 g, 29.5 mmol) was dissolved in dry DCM (50 mL) and mixture was cooled toward −78 °C. Subsequently, 1 M BBr_3 in DCM (59 mL, 59 mmol) was added dropwise over approximately 30 min. The dry-ice acetone bath was removed and the mixture allowed to warm toward room temperature and was stirred overnight. The reaction mixture was then quenched and diluted with water and extracted with MTBE. The organic phase was washed with brine (1×) and dried over $MgSO_4$. The crude was filtered after which remaining volatiles were evaporated in vacuo. The resulting crude was recrystallized from a DCM/MTBE mixture, yielding the product as a white solid.

General Method G: O-Alkylation of Demethylated Pyrazolones. Pyrazolone **65** (500 mg, 1.5 mmol) was dissolved in dry DMF (5 mL) and Cs_2CO_3 (1.0 g, 3.1 mmol) was added followed by (bromomethyl)cyclobutane (0.19 mL, 1.7 mmol). The reaction mixture was stirred for 3 h at room temperature after which the mixture was poured in 30 mL of water. The aqueous phase was extracted with EtOAc after which the organic phase was washed twice with water followed by brine (1×). The organic phase was dried over $MgSO_4$, filtered, and evaporated to dryness. The resulting crude was purified over SiO_2 using a gradient of 20% EtOAc in heptane toward 50% EtOAc in heptane. Evaporation of pure fractions yielded the desired product as a white solid.

Below the experimental details of key-compounds **7**, **8**, **11**, **34**, **65**, **67**, and **76** are included, which are representative for each reaction step. Details as well as the original spectra of all other compounds can be found in the Supporting Information.

Experimental Data. *Methyl 3-(3-Bromo-4-methoxyphenyl)-2,2-dimethyl-3-oxopropanoate (**7**).* Prepared according to general method A. Crude yield: 38 g. Small portion was purified to obtain analysis data. ^{1}H NMR (500 MHz, $CDCl_3$): δ 8.11 (s, 1H), 7.75 (d, J = 8.7 Hz, 1H), 6.88 (d, J = 8.7 Hz, 1H), 3.95 (s, 3H), 3.65 (s, 3H), 1.52 (s, 6H). ^{13}C NMR (126 MHz, $CDCl_3$): δ 194.9, 175.5, 159.2, 134.4, 129.6, 128.8, 112.1, 110.9, 56.5, 53.0, 52.7, 24.0. LC−MS (ESI) no mass observed; retention time: 4.84 min.

*5-(3-Bromo-4-methoxyphenyl)-4,4-dimethyl-2,4-dihydro-3H-pyrazol-3-one (**8**).* Prepared according to general method B starting from crude **7** to afford 22.2 g (75 mmol, 94% over two steps) of the title compound as a white solid. ^{1}H NMR (500 MHz, DMSO-d_6): δ 11.54 (s, 1H), 7.96 (d, J = 2.2 Hz, 1H), 7.77 (dd, J = 8.6, 2.2 Hz, 1H), 7.16 (d, J = 8.7 Hz, 1H), 3.89 (s, 3H), 1.34 (s, 6H). ^{13}C NMR (126 MHz, DMSO): δ 181.0, 160.6, 156.8, 130.3, 127.3, 125.3, 113.1, 111.8, 56.9, 46.8, 22.3. LC−MS (ESI) m/z: found, 297 $[M + H]^+$; retention time, 4.51 min.

*5-(3-Bromo-4-methoxyphenyl)-2-isopropyl-4,4-dimethyl-2,4-dihydro-3H-pyrazol-3-one (**11**).* Prepared according to general method C using 2-bromopropane (0.95 mL, 10 mmol) to afford 2.0 g (5.9 mmol, 70%) of the title compound as a white solid. ^{1}H NMR (500 MHz, $CDCl_3$): δ 8.06 (d, J = 2.0 Hz, 1H), 7.68 (dd, J = 9.0 Hz, 2.0 Hz, 1H), 6.91 (d, J = 8.5 Hz, 1H), 4.50 (h, J = 6.5 Hz, 1H), 3.94 (s, 3H), 1.44 (s, 6H), 1.36

DOI: 10.1021/acsomega.8b02847
ACS Omega 2019, 4, 6585−6596

(d, J = 7.0 Hz, 6H). ^{13}C NMR (126 MHz, $CDCl_3$): δ 177.7, 160.1, 156.9, 131.2, 126.5, 125.2, 112.3, 111.5, 56.4, 48.7, 45.3, 22.6, 20.8. LC−MS (ESI) m/z: found, 339 $[M + H]^+$; retention time, 5.39 min. HRMS-ESI: $[M + H]^+$ calcd for $C_{15}H_{20}BrN_2O_2^+$, 339.0703; found, 339.0700.

*2-Isopropyl-5-(4-methoxy-3-(pyridin-3-yl)phenyl)-4,4-dimethyl-2,4-dihydro-3H-pyrazol-3-one (**34**).* Prepared according to general method D using pyridine-3-ylboronic acid (0.47 g, 3.8 mmol) to afford 650 mg (1.93 mmol, 65%) of the title compound as a white solid. ^{1}H NMR (600 MHz, $CDCl_3$): δ 8.79 (s, 1H), 8.60 (s, 1H), 7.90 (d, J = 7.4 Hz, 1H), 7.83 (d, J = 2.2 Hz, 1H), 7.78 (dd, J = 8.6, 2.0 Hz, 1H), 7.39 (s, 1H), 7.03 (d, J = 8.7 Hz, 1H), 4.50 (hept, J = 6.7 Hz, 1H), 3.87 (s, 3H), 1.48 (s, 6H), 1.36 (d, J = 6.7 Hz, 6H). ^{13}C NMR (151 MHz, $CDCl_3$): δ 177.7, 161.0, 157.7, 149.8, 147.9, 137.2, 133.9, 128.7, 127.6, 127.5, 124.4, 123.2, 111.2, 55.8, 48.8, 45.3, 22.7, 20.8. LC−MS (ESI) m/z: found, 338 $[M + H]^+$; retention time, 3.44 min. HRMS-ESI $[M + H]^+$: calcd for $C_{20}H_{24}N_3O_2^+$, 338.1863; found, 338.1851.

*5-(3-Bromo-4-hydroxyphenyl)-2-isopropyl-4,4-dimethyl-2,4-dihydro-3H-pyrazol-3-one (**65**).* Prepared according to general method F using 1 M BBr_3 in DCM to afford 8.2 g (25.2 mmol, 86%) of the title compound as a white solid. ^{1}H NMR (500 MHz, $CDCl_3$): δ 7.97 (d, J = 2.0 Hz, 1H), 7.64 (dd, J = 8.6, 2.1 Hz, 1H), 7.06 (d, J = 8.6 Hz, 1H), 6.15 (s, 1H), 4.50 (hept, J = 6.7 Hz, 1H), 1.45 (s, 6H), 1.36 (d, J = 6.7 Hz, 6H). ^{13}C NMR (126 MHz, $CDCl_3$): δ 177.8, 160.3, 153.7, 130.1, 127.1, 125.3, 116.2, 110.9, 48.8, 45.4, 22.5, 20.8. LC−MS (ESI) m/z: found, 325 $[M + H]^+$; retention time, 4.87 min. HRMS-ESI: $[M + H]^+$ calcd for $C_{14}H_{18}BrN_2O_2^+$, 325.0546; found, 325.0531.

*5-(3-Bromo-4-isopropoxyphenyl)-2-isopropyl-4,4-dimethyl-2,4-dihydro-3H-pyrazol-3-one (**67**).* Prepared according to general method G using 2-bromopropane (0.16 mL, 1.7 mmol) to afford 510 mg (1.4 mmol, 90%) of the title compound as a white solid. ^{1}H NMR (500 MHz, $CDCl_3$): δ 8.02 (d, J = 2.2 Hz, 1H), 7.64 (dd, J = 8.6, 2.2 Hz, 1H), 6.90 (d, J = 8.7 Hz, 1H), 4.60 (hept, J = 6.0 Hz, 1H), 4.48 (hept, J = 6.7 Hz, 1H), 1.43 (s, 6H), 1.39 (d, J = 6.1 Hz, 6H), 1.34 (d, J = 6.7 Hz, 6H). ^{13}C NMR (126 MHz, $CDCl_3$): δ 177.7, 160.2, 155.6, 131.3, 126.2, 125.0, 114.6, 113.9, 72.1, 48.7, 45.2, 22.6, 22.0, 20.8. LC−MS (ESI) m/z: found, 367 $[M + H]^+$; retention time, 5.54 min. HRMS-ESI: $[M + H]^+$ calcd for $C_{17}H_{24}BrN_2O_2$, 367.1016; found, 367.1012.

*5-(4-Isopropoxy-3-(pyridin-3-yl)phenyl)-2-isopropyl-4,4-dimethyl-2,4-dihydro-3H-pyrazol-3-one (**76**).* Prepared according to general method D using pyridin-3-ylboronic acid (87 mg, 0.71 mmol) to afford 162 mg (0.44 mmol, 81%) of the title compound as a transparent oil which solidified over time. ^{1}H NMR (500 MHz, $CDCl_3$): δ 8.81 (broad singlet, 1H), 8.58 (d, J = 3.8 Hz, 1H), 7.88 (d, J = 7.9 Hz, 1H), 7.82 (d, J = 2.3 Hz, 1H), 7.76 (dd, J = 8.7, 2.3 Hz, 1H), 7.36 (dd, J = 7.8, 4.8 Hz, 1H), 7.02 (d, J = 8.7 Hz, 1H), 4.62 (hept, J = 6.0 Hz, 1H), 4.51 (hept, J = 6.7 Hz, 1H), 1.48 (s, 6H), 1.36 (d, J = 6.7 Hz, 6H), 1.31 (d, J = 6.1 Hz, 6H). ^{13}C NMR (126 MHz, $CDCl_3$): δ 177.7, 161.1, 156.1, 150.2, 148.1, 136.9, 134.0, 128.8, 128.4, 127.3, 124.0, 122.9, 113.7, 70.8, 48.8, 45.2, 22.7, 21.9, 20.8. LC−MS (ESI) m/z: found, 366 $[M + H]^+$; retention time, 3.92 min. HRMS-ESI: $[M + H]^+$ calcd for $C_{22}H_{28}N_3O_2$, 366.2176; found, 366.2185.

■ ASSOCIATED CONTENT

Supporting Information

The Supporting Information is available free of charge on the ACS Publications website at DOI: 10.1021/acsomega.8b02847.

Detailed pharmacological and parasitological data as well as tables of physical chemical properties of synthesized compounds; correlation between physical chemical properties with parasite growth inhibition; detailed experimental data for the compounds **9**−**10**, **12**−**33**, **35**−**64**, **66**, **68**−**74**, **75** and **77**−**83**; and NMR data files of all compounds (PDF)

■ AUTHOR INFORMATION

Corresponding Author

*E-mail: r.leurs@vu.nl (R.L.).

ORCID

Rob Leurs: 0000-0003-1354-2848

Author Contributions

Performing experimental work: Maarten Sijm, K.M.O., J.S.d.A., S.S., A.M., T.v.d.M., P.S., H.C., and I.C.; writing manuscript: M.S., M.d.N.C.S, R.L.; experimental design: M.S., E.E., Marco Siderius, L.M., D.G.B., J.J.M., M.d.N.C.S, G.S., I.J.P.d.E., and R.L.; funding: L.M., D.G.B., M.d.N.C.S, G.S., I.J.P.d.E., and R.L.; reviewing and editing manuscript: M.S., M.d.N.C.S, G.S., and R.L. All authors have given approval to the final version of the manuscript.

Funding

The PDE4NPD project was funded by the European Union under the FP-7-Health program, project ID: 602666. MNCS is a researcher with the CNPq and CNE/FAPERJ.

Notes

The authors declare no competing financial interest.

■ ACKNOWLEDGMENTS

The authors would like to thank all other members of PDE4NPD for insightful discussions and helpful comments. Furthermore, we thank Stijn Laan, Krishnili Ramratan, Amid Sangar, Eakta Singh, and Ruth Willems for their assistance on the synthesis.

■ LIST OF ABBREVIATIONS

a.a., amino acid; bs, broad singlet, BT: bloodstream trypomastigotes; cAMP, cyclic adenosine monophosphate; CD, catalytic domain; cGMP, cyclic guanosine monophosphate; clog P, calculated logarithm of the partition-coefficient; CYP51, cytochorome P450 51; d, doublet; DCM, dichloromethane; dd, double doublet; DME, dimethoxyethane; dt, double triplet; DTU, discrete typing units; DMF, dimethylformamide; dppf, 1,1′-ferrocenediyl-bis(diphenylphosphine); DTT, dithiothreitol; EDTA, ethylenediaminetetraacetic acid; ESI, electron spray ionization; EtOAc, ethylacetate; FCS, fetal calf serum; FPMK, fragments per kilobase of transcript per million mapped reads; q, quartet; h, heptet; HRMS, high-resolution mass spectroscopy; HTS, high-throughput screening; Hz, hertz; J, coupling constant; IC, intracellular; LC−MS, liquid chromatography-mass spectroscopy; LDA, lithium di-isopropyl amide; m, multiplet; MeOH, methanol; MHz, megahertz; MRC-5, medical research council cell strain 5; mRNA, messenger RNA; MTBE, methyl *tert*-butyl ether; NMR, nuclear magnetic resonance; p, pentet;

DOI: 10.1021/acsomega.8b02847
ACS Omega 2019, 4, 6585−6596

PDE, phosphodiesterase; q, quartet; RLU, relative light unit; s, singlet; SAR, structure−activity relationship; SEM, standard error of the mean; t, triplet; Tbr, *Trypanosoma brucei*; Tcr, *Trypanosoma cruzi*; THF, tetrahydrofuan; TPSA, topical polar surface area

REFERENCES

(1) Schmunis, G. Trypanosoma cruzi, the etiologic agent of Chagas' disease: status in the blood supply in endemic and nonendemic countries. *Transfusion* **1991**, *31*, 547−557.

(2) Bern, C.; Montgomery, S. P. An Estimate of the Burden of Chagas Disease in the United States. *Clin. Infect. Dis.* **2009**, *49*, e52−e54.

(3) Bern, C.; Kjos, S.; Yabsley, M. J.; Montgomery, S. P. Trypanosoma cruzi and Chagas' Disease in the United States. *Clin. Microbiol. Rev.* **2011**, *24*, 655−681.

(4) Coura, J. R.; Viñas, P. A. Chagas disease: a new worldwide challenge. *Nature* **2010**, *465*, S6−S7.

(5) Schmunis, G. A.; Yadon, Z. E. Chagas disease: A Latin American health problem becoming a world health problem. *Acta Trop.* **2010**, *115*, 14−21.

(6) http://www.dndi.org/diseases-projects/diseases/chagas.html (Dec 12, 2015).

(7) WHO. Chagas disease (American trypanosomiasis). http://www.who.int/mediacentre/factsheets/fs340/en/ (Nov 05, 2018).

(8) Urbina, J. A.; Docampo, R. Specific chemotherapy of Chagas disease: controversies and advances. *Trends Parasitol.* **2003**, *19*, 495−501.

(9) Morillo, C. A.; Marin-Neto, J. A.; Avezum, A.; Sosa-Estani, S.; Rassi, A.; Rosas, F.; Villena, E.; Quiroz, R.; Bonilla, R.; Britto, C.; Guhl, F.; Velazquez, E.; Bonilla, L.; Meeks, B.; Rao-Melacini, P.; Pogue, J.; Mattos, A.; Lazdins, J.; Rassi, A.; Connolly, S. J.; Yusuf, S. Randomized Trial of Benznidazole for Chronic Chagas' Cardiomyopathy. *N. Engl. J. Med.* **2015**, *373*, 1295−1306.

(10) Castro, J. A.; deMecca, M. M.; Bartel, L. C. Toxic Side Effects of Drugs Used to Treat Chagas' Disease (American Trypanosomiasis). *Hum. Exp. Toxicol.* **2006**, *25*, 471−479.

(11) Zingales, B.; Araujo, R. G. A.; Moreno, M.; Franco, J.; Aguiar, P. H. N.; Nunes, S. L.; Silva, M. N.; Ienne, S.; Machado, C. R.; Brandão, A. A novel ABCG-like transporter of Trypanosoma cruzi is involved in natural resistance to benznidazole. *Memórias do Inst. Oswaldo Cruz* **2015**, *110*, 433−444.

(12) Rogers, N. Bugging out over Chagas: Bioluminescent protozoans and old drugs might help unravel kissing-bug disease. *Nat. Med.* **2015**, *21*, 1108−1110.

(13) Cerecetto, H.; González, M. Synthetic Medicinal Chemistry in Chagas' Disease: Compounds at The Final Stage of "Hit-To-Lead" Phase. *Pharmaceuticals* **2010**, *3*, 810−838.

(14) Khare, S.; Nagle, A. S.; Biggart, A.; Lai, Y. H.; Liang, F.; Davis, L. C.; Barnes, S. W.; Mathison, C. J. N.; Myburgh, E.; Gao, M.-Y.; Gillespie, J. R.; Liu, X.; Tan, J. L.; Stinson, M.; Rivera, I. C.; Ballard, J.; Yeh, V.; Groessl, T.; Federe, G.; Koh, H. X. Y.; Venable, J. D.; Bursulaya, B.; Shapiro, M.; Mishra, P. K.; Spraggon, G.; Brock, A.; Mottram, J. C.; Buckner, F. S.; Rao, S. P. S.; Wen, B. G.; Walker, J. R.; Tuntland, T.; Molteni, V.; Glynne, R. J.; Supek, F. Proteasome inhibition for treatment of leishmaniasis, Chagas disease and sleeping sickness. *Nature* **2016**, *537*, 229−233.

(15) Peña, I.; Pilar Manzano, M.; Cantizani, J.; Kessler, A.; Alonso-Padilla, J.; Bardera, A. I.; Alvarez, E.; Colmenarejo, G.; Cotillo, I.; Roquero, I.; de Dios-Anton, F.; Barroso, V.; Rodriguez, A.; Gray, D. W.; Navarro, M.; Kumar, V.; Sherstnev, A.; Drewry, D. H.; Brown, J. R.; Fiandor, J. M.; Julio Martin, J. New Compound Sets Identified from High Throughput Phenotypic Screening Against Three Kinetoplastid Parasites: An Open Resource. *Sci. Rep.* **2015**, *5*, 8771.

(16) Keravis, T.; Lugnier, C. Cyclic nucleotide phosphodiesterase (PDE) isozymes as targets of the intracellular signalling network: benefits of PDE inhibitors in various diseases and perspectives for future therapeutic developments. *Br. J. Pharmacol.* **2012**, *165*, 1288−1305.

(17) Maurice, D. H.; Ke, H.; Ahmad, F.; Wang, Y.; Chung, J.; Manganiello, V. C. Advances in targeting cyclic nucleotide phosphodiesterases. *Nat. Rev. Drug Discov.* **2014**, *13*, 290−314.

(18) Mancini, P.; Patton, C. Cyclic 3′,5′-adenosine monophosphate levels during the developmental cycle of Trypanosoma brucei brucei in the rat. *Mol. Biochem. Parasitol.* **1981**, *3*, 19−31.

(19) Rangel-Aldao, R.; Allende, O.; Triana, F.; Piras, R.; Henriquez, D.; Piras, M. Possible role of cAMP in the differentiation of Trypanosoma cruzi. *Mol. Biochem. Parasitol.* **1987**, *22*, 39−43.

(20) Kunz, S.; Beavo, J. A.; D'Angelo, M. A.; Flawia, M. M.; Francis, S. H.; Johner, A.; Laxman, S.; Oberholzer, M.; Rascon, A.; Shakur, Y.; Wentzinger, L.; Zoraghi, R.; Seebeck, T. Cyclic nucleotide specific phosphodiesterases of the kinetoplastida: A unified nomenclature. *Mol. Biochem. Parasitol.* **2006**, *145*, 133−135.

(21) Orrling, K. M.; Jansen, C.; Vu, X. L.; Balmer, V.; Bregy, P.; Shanmugham, A.; England, P.; Bailey, D.; Cos, P.; Maes, L.; Adams, E.; van den Bogaart, E.; Chatelain, E.; Ioset, J.-R.; van de Stolpe, A.; Zorg, S.; Veerman, J.; Seebeck, T.; Sterk, G. J.; de Esch, I. J. P.; Leurs, R. Catechol Pyrazolinones as Trypanocidals: Fragment-Based Design, Synthesis, and Pharmacological Evaluation of Nanomolar Inhibitors of Trypanosomal Phosphodiesterase B1. *J. Med. Chem.* **2012**, *55*, 8745−8756.

(22) Jansen, C.; Wang, H.; Kooistra, A. J.; de Graaf, C.; Orrling, K. M.; Tenor, H.; Seebeck, T.; Bailey, D.; de Esch, I. J. P.; Ke, H.; Leurs, R. Discovery of Novel Trypanosoma brucei Phosphodiesterase B1 Inhibitors by Virtual Screening against the Unliganded TbrPDEB1 Crystal Structure. *J. Med. Chem.* **2013**, *56*, 2087−2096.

(23) Kunz, S.; Balmer, V.; Sterk, G. J.; Pollastri, M. P.; Leurs, R.; Müller, N.; Hemphill, A.; Spycher, C. The single cyclic nucleotide-specific phosphodiesterase of the intestinal parasite Giardia lamblia represents a potential drug target. *PLoS Neglected Trop. Dis.* **2017**, *11*, e0005891.

(24) de Koning, H. P.; Gould, M. K.; Sterk, G. J.; Tenor, H.; Kunz, S.; Luginbuehl, E.; Seebeck, T. Pharmacological Validation of Trypanosoma brucei Phosphodiesterases as Novel Drug Targets. *J. Infect. Dis.* **2012**, *206*, 229−237.

(25) Veerman, J.; van den Bergh, T.; Orrling, K. M.; Jansen, C.; Cos, P.; Maes, L.; Chatelain, E.; Ioset, J.-R.; Edink, E. E.; Tenor, H.; Seebeck, T.; de Esch, I.; Leurs, R.; Sterk, G. J. Synthesis and evaluation of analogs of the phenylpyridazinone NPD-001 as potent trypanosomal TbrPDEB1 phosphodiesterase inhibitors and in vitro trypanocidals. *Bioorg. Med. Chem.* **2016**, *24*, 1573−1581.

(26) Makin, L.; Gluenz, E. cAMP signalling in trypanosomatids: role in pathogenesis and as a drug target. *Trends Parasitol.* **2015**, *31*, 373−379.

(27) Rohloff, P.; Montalvetti, A.; Docampo, R. Acidocalcisomes and the Contractile Vacuole Complex Are Involved in Osmoregulation inTrypanosoma cruzi. *J. Biol. Chem.* **2004**, *279*, 52270−52281.

(28) Rohloff, P.; Rodrigues, C. O.; Docampo, R. Regulatory volume decrease in Trypanosoma cruzi involves amino acid efflux and changes in intracellular calcium. *Mol. Biochem. Parasitol.* **2003**, *126*, 219−230.

(29) King-Keller, S.; Li, M.; Smith, A.; Zheng, S.; Kaur, G.; Yang, X.; Wang, B.; Docampo, R. Chemical Validation of Phosphodiesterase C as a Chemotherapeutic Target in Trypanosoma cruzi, the Etiological Agent of Chagas' Disease. *Antimicrob. Agents Chemother.* **2010**, *54*, 3738−3745.

(30) Riley, J.; Brand, S.; Voice, M.; Caballero, I.; Calvo, D.; Read, K. D. Development of a Fluorescence-based *Trypanosoma cruzi* CYP51 Inhibition Assay for Effective Compound Triaging in Drug Discovery Programmes for Chagas Disease. *PLoS Neglected Trop. Dis.* **2015**, *9*, e0004014.

(31) Wang, H.; Kunz, S.; Chen, G.; Seebeck, T.; Wan, Y.; Robinson, H.; Martinelli, S.; Ke, H. Biological and Structural Characterization ofTrypanosoma cruziPhosphodiesterase C and Implications for Design of Parasite Selective Inhibitors. *J. Biol. Chem.* **2012**, *287*, 11788−11797.

DOI: 10.1021/acsomega.8b02847
ACS Omega 2019, 4, 6585−6596

(32) Gunatilleke, S. S.; Calvet, C. M.; Johnston, J. B.; Chen, C.-K.; Erenburg, G.; Gut, J.; Engel, J. C.; Ang, K. K. H.; Mulvaney, J.; Chen, S.; Arkin, M. R.; McKerrow, J. H.; Podust, L. M. Diverse Inhibitor Chemotypes Targeting *Trypanosoma cruzi* CYP51. *PLoS Neglected Trop. Dis.* **2012**, *6*, e1736.
(33) Li, Y.; Shah-Simpson, S.; Okrah, K.; Belew, A. T.; Choi, J.; Caradonna, K. L.; Padmanabhan, P.; Ndegwa, D. M.; Temanni, M. R.; Corrada Bravo, H.; El-Sayed, N. M.; Burleigh, B. A. Transcriptome Remodeling in Trypanosoma cruzi and Human Cells during Intracellular Infection. *PLoS Pathog.* **2016**, *12*, e1005511.
(34) Tagoe, D. N. A.; Kalejaiye, T. D.; de Koning, H. P. The ever unfolding story of cAMP signaling in trypanosomatids: vive la difference! *Front. Pharmacol.* **2015**, *6*, 185.
(35) Andriani, G.; Amata, E.; Beatty, J.; Clements, Z.; Coffey, B. J.; Courtemanche, G.; Devine, W.; Erath, J.; Juda, C. E.; Wawrzak, Z.; Wood, J. T.; Lepesheva, G. I.; Rodriguez, A.; Pollastri, M. P. Antitrypanosomal Lead Discovery: Identification of a Ligand-Efficient Inhibitor of Trypanosoma cruzi CYP51 and Parasite Growth. *J. Med. Chem.* **2013**, *56*, 2556−2567.
(36) Lepesheva, G. I.; Hargrove, T. Y.; Anderson, S.; Kleshchenko, Y.; Furtak, V.; Wawrzak, Z.; Villalta, F.; Waterman, M. R. Structural Insights into Inhibition of Sterol 14α-Demethylase in the Human PathogenTrypanosoma cruzi. *J. Biol. Chem.* **2010**, *285*, 25582−25590.
(37) Soeiro, M. d. N. C.; de Souza, E. M.; da Silva, C. F.; Batista, D. d. G. J.; Batista, M. M.; Pavão, B. P.; Araújo, J. S.; Aiub, C. A. F.; da Silva, P. B.; Lionel, J.; Britto, C.; Kim, K.; Sulikowski, G.; Hargrove, T. Y.; Waterman, M. R.; Lepesheva, G. I. In VitroandIn VivoStudies of the Antiparasitic Activity of Sterol 14α-Demethylase (CYP51) Inhibitor VNI against Drug-Resistant Strains of Trypanosoma cruzi. *Antimicrob. Agents Chemother.* **2013**, *57*, 4151−4163.
(38) Molina, I.; Gómez i Prat, J.; Salvador, F.; Treviño, B.; Sulleiro, E.; Serre, N.; Pou, D.; Roure, S.; Cabezos, J.; Valerio, L.; Blanco-Grau, A.; Sánchez-Montalvá, A.; Vidal, X.; Pahissa, A. Randomized Trial of Posaconazole and Benznidazole for Chronic Chagas' Disease. *N. Engl. J. Med.* **2014**, *370*, 1899−1908.
(39) Saccoliti, F.; Madia, V. N.; Tudino, V.; De Leo, A.; Pescatori, L.; Messore, A.; De Vita, D.; Scipione, L.; Brun, R.; Kaiser, M.; Mäser, P.; Calvet, C. M.; Jennings, G. K.; Podust, L. M.; Pepe, G.; Cirilli, R.; Faggi, C.; Di Marco, A.; Battista, M. R.; Summa, V.; Costi, R.; Di Santo, R. Design, Synthesis, and Biological Evaluation of New 1-(Aryl-1H-pyrrolyl)(phenyl)methyl-1H-imidazole Derivatives as Antiprotozoal Agents. *J. Med. Chem.* **2019**, *62*, 1330−1347.
(40) Villalta, F.; Dobish, M. C.; Nde, P. N.; Kleshchenko, Y. Y.; Hargrove, T. Y.; Johnson, C. A.; Waterman, M. R.; Johnston, J. N.; Lepesheva, G. I. VNI Cures Acute and Chronic Experimental Chagas Disease. *J. Infect. Dis.* **2013**, *208*, 504−511.
(41) Molina, I.; Salvador, F.; Sánchez-Montalvá, A. The use of posaconazole against Chagas disease. *Curr. Opin. Infect. Dis.* **2015**, *28*, 397−407.
(42) Lepesheva, G. I.; Friggeri, L.; Waterman, M. R. CYP51 as drug targets for fungi and protozoan parasites: past, present and future. *Parasitology* **2018**, *145*, 1820−1836.
(43) Guedes-da-Silva, F. H.; Batista, D. G. J.; Da Silva, C. F.; De Araújo, J. S.; Pavão, B. P.; Simões-Silva, M. R.; Batista, M. M.; Demarque, K. C.; Moreira, O. C.; Britto, C.; Lepesheva, G. I.; Soeiro, M. N. C. Antitrypanosomal Activity of Sterol 14α-Demethylase (CYP51) Inhibitors VNI and VFV in the Swiss Mouse Models of Chagas Disease Induced by the Trypanosoma cruzi Y Strain. *Antimicrob. Agents Chemother.* **2017**, *61*, e02098-16.
(44) Chatelain, E.; Ioset, J.-R. Phenotypic screening approaches for Chagas disease drug discovery. *Expert Opin. Drug Discov.* **2018**, *13*, 141−153.
(45) Lepesheva, G. I.; Hargrove, T. Y.; Rachakonda, G.; Wawrzak, Z.; Pomel, S.; Cojean, S.; Nde, P. N.; Nes, W. D.; Locuson, C. W.; Calcutt, M. W.; Waterman, M. R.; Daniels, J. S.; Loiseau, P. M.; Villalta, F. VFV as a New Effective CYP51 Structure-Derived Drug Candidate for Chagas Disease and Visceral Leishmaniasis. *J. Infect. Dis.* **2015**, *212*, 1439−1448.
(46) Higuera, S. L.; Guhl, F.; Ramírez, J. Identification of Trypanosoma cruzi Discrete Typing Units (DTUs) through the implementation of a High-Resolution Melting (HRM) genotyping assay. *Parasites Vectors* **2013**, *6*, 112.
(47) Hargrove, T. Y.; Wawrzak, Z.; Alexander, P. W.; Chaplin, J. H.; Keenan, M.; Charman, S. A.; Perez, C. J.; Waterman, M. R.; Chatelain, E.; Lepesheva, G. I. Complexes ofTrypanosoma cruziSterol 14α-Demethylase (CYP51) with Two Pyridine-based Drug Candidates for Chagas Disease. *J. Biol. Chem.* **2013**, *288*, 31602−31615.
(48) Meirelles, M. N.; de Araujo-Jorge, T. C.; Miranda, C. F.; de Souza, W.; Barbosa, H. S. Interaction of *Trypanosoma cruzi* with heart muscle cells: ultrastructural and cytochemical analysis of endocytic vacuole formation and effect upon myogenesis in vitro. *Eur. J. Cell Biol.* **1986**, *41*, 198.
(49) Batista, D. d. G. J.; Batista, M. M.; Oliveira, G. M. d.; Amaral, P. B. d.; Lannes-Vieira, J.; Britto, C. C.; Junqueira, A.; Lima, M. M.; Romanha, A. J.; Sales Junior, P. A.; Stephens, C. E.; Boykin, D. W.; Soeiro, M. d. N. C. Arylimidamide DB766, a Potential Chemotherapeutic Candidate for Chagas' Disease Treatment. *Antimicrob. Agents Chemother.* **2010**, *54*, 2940−2952.
(50) Timm, B. L.; da Silva, P. B.; Batista, M. M.; da Silva, F. H. G.; da Silva, C. F.; Tidwell, R. R.; Patrick, D. A.; Jones, S. K.; Bakunov, S. A.; Bakunova, S. M.; Soeiro, M. d. N. C. In VitroandIn VivoBiological Effects of Novel Arylimidamide Derivatives against Trypanosoma cruzi. *Antimicrob. Agents Chemother.* **2014**, *58*, 3720−3726.

DOI: 10.1021/acsomega.8b02847
ACS Omega 2019, 4, 6585−6596